Robotica (2009) volume 27, pp. 469–479. © 2008 Cambridge University Press
doi:10.1017/S0263574708004840 Printed in the United Kingdom

Fast laser scan matching approach based on adaptive curvature estimation for mobile robots

P. Núñez†*, R. Vázquez-Martín‡, A. Bandera‡ and F. Sandoval‡

†*Grupo de Telecomunicaciones, Dept. Tecnología de los Computadores y las Comunicaciones, Universidad de Extremadura, Cáceres, Spain.*
‡*Grupo de Ingeniería de Sistemas Integrados, Dept. Tecnología Electrónica, Universidad de Málaga, 29071-Málaga, Spain.*

(Received in Final Form: May 29, 2008. First published online: July 7, 2008)

SUMMARY
This paper describes a complete laser-based approach for tracking the pose of a robot in a dynamic environment. The main novelty of this approach is that the matching between consecutively acquired scans is achieved using their associated curvature-based representations. The proposed scan matching algorithm consists of three stages. Firstly, the whole raw laser data is segmented into groups of consecutive range readings using a distance-based criterion and the curvature function for each group is computed. Then, this set of curvature functions is matched to the set of curvature functions associated to the previously acquired laser scan. Finally, characteristic points of pairwise curvature functions are matched and used to correctly obtain the best local alignment between consecutive scans. A closed form solution is employed for computing the optimal transformation and minimizing the robot pose shift error without iterations. Thus, the system is outstanding in terms of accuracy and computation time. The implemented algorithm is evaluated and compared to three state of the art scan matching approaches.

KEYWORDS: Scan matching, Adaptive curvature function, Mobile robotics.

1. Introduction

One of the key functions in an autonomous mobile robot is to keep track of its pose—position and orientation—while moving. To achieve this relative localization and to reduce the increasing error from the use of dead reckoning, it is common that the robot carries external sensors, like a 2-D laser range finders, to perceive the environment. Environment perceptions taken from different locations and instants of time could be matched and then it would be possible to update the position estimate according to the matching results. It can be noted that the goal of this matching process would not be directly to build an accurate map, but rather to ensure a stable and fast localization, regardless of the robot speed and without any restrictions of the covered distance.[9] To achieve that, the scan matching techniques estimate the robot displacement between two instants of time by directly comparing the perceived scans. Thus, they can be used, for instance, to improve the performance of navigation approaches which try to solve the simultaneous localization and mapping (SLAM) problem. The SLAM problem has received considerable attention over the last decade and different solutions have been proposed.[3,6,11] The difficulty of the SLAM approach lies in the fact that an accurate estimation of the robot trajectory is required to obtain a good map. As has been pointed out by several authors, it is possible to reduce the localization error due to slippage using scan matching algorithms as an improved odometry.[8,12,15]

One of the main differences between the existing scan matching algorithms is their usage and not their features extracted from the raw data, as line segments or corners.[9] Thus, in structured environment it can be assumed that the existence of polygonal elements can be extracted from the data and can be used to align the scans.[5,7] These methods are efficient and reliable and, therefore, they have been widely used to provide robot self-localization in these environments. However, these geometric items are not present in unstructured environments. To deal with these situations, a second category of raw data matching techniques which work without explicit geometric interpretation has been developed.[14,16] However, most of these point-to-point methods have been designed for situations in which the environment is static during the measurement process. Therefore, dynamic items (e.g. people or objects moving around the robot) can lead to serious errors in the pose estimation.[2]

Independently of the chosen strategy, it would be desirable that a scan matching algorithm handle the following three demands[2]:

1. Eliminate scan points associated to dynamic objects in the environment or otherwise the result will be incorrect.
2. Match in structured and unstructured environments.
3. Provide information about the uncertainty of the estimated robot pose.

This paper proposes a novel scan matching approach based on the curvature information associated to the scan (named CF-SMA, from *Curvature Function—Scan Matching Algorithm*). This algorithm can deal with dynamic, structured or unstructured environments. Besides, it obtains

* Corresponding author. E-mail: pmnt@uma.es

https://doi.org/10.1017/S0263574708004840 Published online by Cambridge University Press

an uncertainty matrix for the robot pose. In this approach, the fast and robust correspondence between two consecutive scans is achieved from the matching of characteristic points extracted from pairwise curvature functions. The representation of the laser scan data using a set of adaptively estimated curvature functions was originally proposed by the authors in a previous work.[13] In this paper, this concept is applied to the efficient matching of laser scans. Experimental results show that the performance of the proposed approach is high in terms of precision and computational cost. Thus, the method has been successfully compared to other similar approaches.

2. Proposed Method

Let $p_t^r = (x_t^r, y_t^r, \theta_t^r)^T$ be the t-th pose of the robot, where (x_t^r, y_t^r) are the co-ordinates in the XY horizontal-frontal plane and θ_t^r is the orientation with respect to the vertical axis Z. The aim of scan matching approach is to calculate an estimation of the robot displacement between two different instants of time by comparing consecutive scans provided by a laser range finder. This relative displacement, $\Delta p^r = (\Delta x^r, \Delta y^r, \Delta\theta^r)^T$, can be used to update the robot pose and, therefore to provide an alternative source of information to the robot odometry (in fact, this relative displacement will be usually more reliable than the odometric information provided by proprioceptive sensors, which could be affected by sliding errors). Given a pose and the estimated relative shift Δp^r, the updated pose p_{t+1}^r can be calculated according to the kinematics model:

$$\begin{pmatrix} x_{t+1}^r \\ y_{t+1}^r \\ \theta_{t+1}^r \end{pmatrix} = \begin{pmatrix} x_t^r \\ y_t^r \\ \theta_t^r \end{pmatrix} + \begin{pmatrix} \cos\theta_t^r & \sin\theta_t^r & 0 \\ -\sin\theta_t^r & \cos\theta_t^r & 0 \\ 0 & 0 & 1 \end{pmatrix} \cdot \begin{pmatrix} \Delta x^r \\ \Delta y^r \\ \Delta\theta^r \end{pmatrix}. \quad (1)$$

The main limitation of scan matching approaches is that the quality of the matching process is crucial for an accurate estimation. In fact, a bad association between two consecutive scans provokes a significant robot pose error which is non-recoverable in most of the situations.[2] Thus, a significant advance in these scan matching algorithms is the possibility of removing those outliers points or features which increases the pose error.

The approach described in this paper proposes a curvature-based scan matching algorithm which removes those features which can increase the robot pose error. As can be noted in Fig. 1, the proposed approach consists of three independent stages. Next, a brief description of the modules depicted in Fig. 1 is provided:

- **CF-SMA1**. At the first stage, the current scan, C, is segmented into groups using a distance-based criterion. Then, the curvature function for each group is computed (see Fig. 1). This curvature function is calculated using an estimator which adapts itself to the local surrounding of the studied range reading. This segmentation process is described with details in a previous work.[13]
- **CF-SMA2**. A correlation matrix which measures the similarity between the sets of curvature functions associated to the current scan and to the previously acquired scan (denoted as reference scan, R) is built. This matrix allows to select pairwise curvature functions and removes isolated groups which will not be included in the robot pose estimate process. In order to perform this calculation in a fast and robust way, the approach implements a FFT algorithm which allows to compare curvature functions only using products. The output of this stage are two subsets of corresponding points, $C' \subseteq C$ and $R' \subseteq R$, which permit to compute the pose shift as the optimal transformation mapping C' onto R'.
- **CF-SMA3**. Finally, the best local alignment between consecutive scans is obtained using C' and R'. Here, a closed form solution is employed for computing the optimal transformation, improving computational time of the scan matching algorithm. Robot's pose is updated according to Eq. (1) and current scan is saved as the new reference scan ($R \longleftarrow C$).

Next subsections present a detailed description of each stage. In order to improve the understanding of the proposed algorithm, Table I summarizes the main symbols used in this paper.

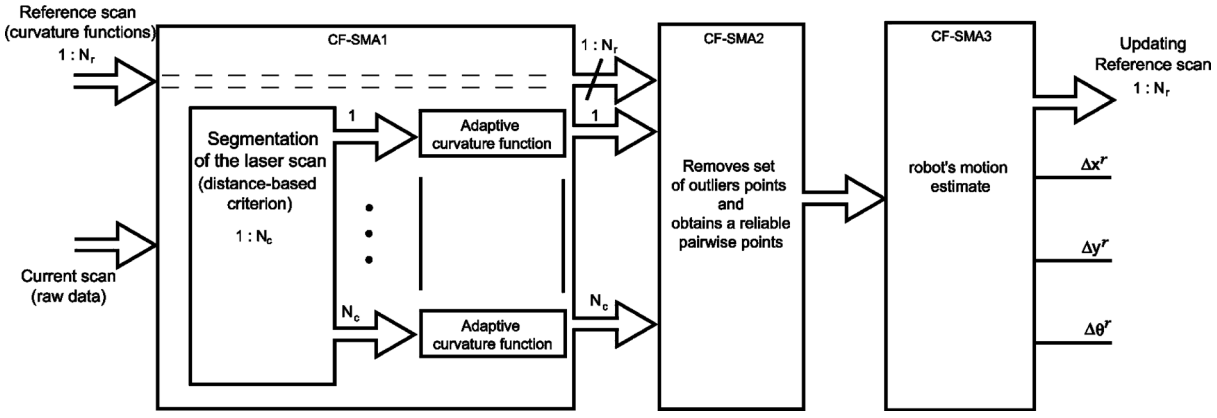


Fig. 1. Overview of the scan matching algorithm proposed in this paper. The method uses three consecutive stages in order to obtain the best alignment between consecutive scans.

https://doi.org/10.1017/S0263574708004840 Published online by Cambridge University Press

Table I. Main symbols used in this paper.

Symbol	Description
$p_t^r = (x^r, y^r, \theta^r)$	Robot's position at time instant t
$\Delta p^r = (\Delta x^r, \Delta y^r, \Delta\theta^r)$	Relative displacement between two consecutive time instants
$(\rho, \varphi)_l$ and $(x, y)_l$	Polar and Cartesian co-ordinates of the l range reading, respectively
σ_ρ^2 and σ_φ^2	Variance of the range and orientation measurement errors (laser range finder)
N_R	Number of data points of the whole scan
C and R	Current and reference scans
N_c and N_r	Number of segments after distance-based segmentation (current and reference scans)
$N_{R_i}^c$ and $N_{R_i}^r$	Number of data points of the i segment (current and reference scans)
k_l	Adaptive k value for calculating the curvature function
η_l	Curvature index associated to the data point l
η_l^i	Curvature index associated to the data point l, which belong to the segment i of the scan
C_{cf} and R_{cf}	Set of curvature functions associated to the scans (current and reference)
P_{cf}	Set of pairwise curvature functions
υ_{ij}	Correlation index between curvature functions $c_i \in C_{cf}$ and $r_j \in R_{cf}$
$\upsilon^{\max}$	Maximum correlation index which describes pairwise curvature functions
N_k	Number of matched curvature functions
$N_{t'}$	Number of possible matched points
N_t	Number of real matched points
N_l	Number of characteristic points
N_l^c and N_l^r	Number of characteristics points for the current and reference scan, respectively
n	Number of point at right and left sides of each characteristic point

2.1. CF-SMA1. Calculation of the set of curvature functions associated to the laser scan

In robotic field, scan data are typically in the form $\{(\rho, \varphi)_{l|l=1\ldots N_R}\}$, on which $(\rho, \varphi)_l$ are the polar co-ordinates of the l-th range reading (ρ_l is the measured distance of an obstacle to the sensor rotating axis at direction φ_l) and N_R is the number of range readings. It is assumed that each range reading is independently affected by Gaussian noise in both co-ordinates, range and bearing, with zero mean and variance σ_ρ^2 and σ_φ^2, respectively. The proposed scan matching approach is based on the matching of physical entities of the scene which are present in both scans. From this matching, the search of pairwise points can be derived. Therefore, it will be necessary to obtain a complete description of the environment which allows to identify a set of distinguished entities. To obtain this description, the scan is firstly segmented using the adaptive breakpoint detector.[4] This detector proposes that two consecutive range readings belong to the same segment if the distance between them is less than a variable threshold, instead of a constant one. Since the sensor angular increment is constant, this threshold will only depend on the range scan distance. The threshold value can be determined from the geometrical scheme shown in Fig. 2. In this figure, it is defined as a virtual line which passes through the scan point ρ_{l-1} making an angle λ with respect to the scanning direction φ_{l-1}. This angle will represent the worst case of incidence angle of the laser scan ray with respect to a line for which range readings are still reliable. Its value will be determined with user experience. Under this constraint, with some assumptions and further mathematical development, the adaptive breakpoint detector specifies that two consecutive range readings belong to different segments if

$$\|(\rho, \varphi)_l - (\rho, \varphi)_{l-1}\| > \rho_{l-1} \cdot \frac{\sin \Delta\varphi}{\sin(\lambda - \Delta\varphi)} + 3\sigma_\rho, \quad (2)$$

where $\Delta\varphi$ is the laser angular resolution, λ is a user-specified constant parameter and σ_ρ the range standard deviation of the sensor measures. The presence of this value in the equation allows to encompass the stochastic behaviour of ρ_l.[4]

Points which belong to the same segment i in the current scan are associated to one element of the environment. If each group of points is characterized by a curvature function, $c_i = \{\eta_l^i \,|\, l = 1, \ldots, N_{R_i}^c\}$, where η_l^i value is the curvature index associated to the range reading l of the segment i, then the whole scan will be described by a set of N_c curvature functions, $C_{cf} = \{c_i \,|\, i = 1, \ldots, N_c\}$. Curvature functions basically describe how much a curve bends at each point. Peaks of the curvature function correspond to the corners of the represented curve and their height depends on the angle at these corners. Flat segments whose average value is larger than zero are related to curve segments and

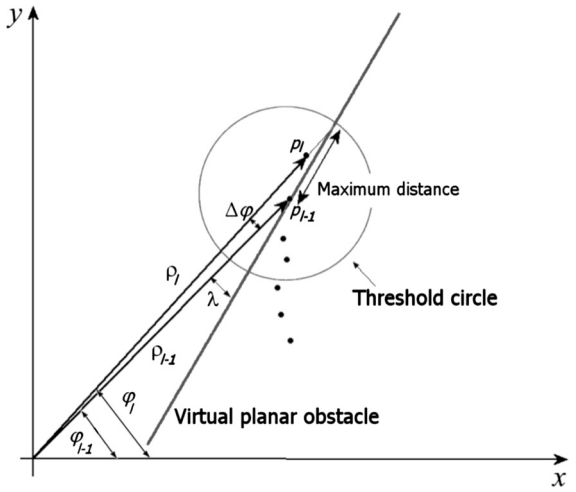


Fig. 2. Geometrical scheme associated to the adaptive breakpoint detector. Section 2.1 explains with details the algorithm.

https://doi.org/10.1017/S0263574708004840 Published online by Cambridge University Press

those whose average value is equal to zero are related to straight line segments. Thus, the curvature function can be used as a descriptor of the current scan segment. In this case, the curvature estimator is a modified version of the adaptive method described in ref. [13]. With respect to the previous version, this new algorithm reduces the computational load characterizing each range reading by a unique value (k_i). In the previous work, the algorithm calculated the maximum lengths of the laser scan presenting no discontinuities on the right and left sides of the range reading (named k_f and k_b, respectively), and used them to obtain two vectors which allowed to calculate the curvature value. Let $\{(x, y)_{l|l=1,\ldots,N_R}\}$ be the Cartesian representation of the range images, where $x_l = \rho_l \cos\varphi_l$ and $y_l = \rho_l \sin\varphi_l$; the method used to calculate the adaptive curvature function for each extracted segment consists of the following steps:

1. Calculation of the maximum length of laser scan presenting no discontinuities on the right side of the working range reading l, k_l. This is obtained as the largest value that satisfies:

$$\sum_{j=l}^{k_l+l-1} d(j, j+1) - d(l, l+k_l) < U_k, \tag{3}$$

where $d(l, j)$ is the Euclidean distance from range reading l to range reading j, and U_k is a threshold value which allows the smoothing of the noise associated to the laser data acquisition. As can be noted in Eq. (3), the k_l value is then adaptively selected according to the surrounding of each range reading l.

2. Estimation of the curvature angle associated to each range reading l, denoted as ϑ_l. According to the previous k_l value, this angle ϑ_l can be obtained as (see Fig. 3):

$$\vartheta_l = \arctan\left(\frac{\sum_{j=l}^{k_l+l-1}(x_{j+1} - x_j)}{\sum_{j=l}^{k_l+l-1}(y_{j+1} - y_j)}\right) \tag{4}$$

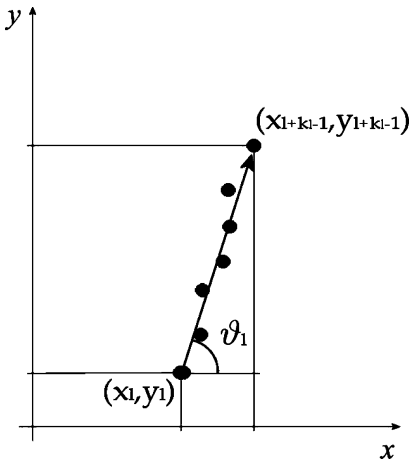


Fig. 3. Calculation of the curvature angle associated to each range reading l, ϑ_l. The maximum length of laser scan presenting no discontinuities on the right side of the working range reading l, k_l, was adaptively estimated according to the surrounding of the range reading l.

3. Calculation of the curvature index associated to each range reading l. This value can be estimated using the equation:

$$\eta_l = \vartheta_{l+1} - \vartheta_{l.} \tag{5}$$

Figure 4a illustrates this segmentation stage for a real scan of a structured environment. As is shown, eight distinct segments are defined in the figure. Isolated group of points are removed using a constraint related to the size of each segment.[13] In Fig. 4b, the absolute value of the curvature functions associated to each scan segment in Fig. 4a is shown.

2.2. CF-SMA2. Points matching from two consecutive scans

As aforementioned, the proposed approach is based on the idea that the tracking of physical entities of the scene can be carried out by matching the sets of curvature functions associated to two successively acquired scans. Thus, C_{cf} is compared to the set of curvature functions from reference scan, R_{cf}. If the number of groups in this reference scan is N_r, and being $N^r_{R_i}$ the number of range readings for each one of these segments, R_{cf} is defined as $R_{cf} = \{r_i \mid i = 1, \ldots, N_r\}$, being $r_i = \{\eta^i_l \mid l = 1, \ldots, N^r_{R_i}\}$. For the sake of efficiency and robustness, instead of considering all the points of the set of pairwise curvature functions, P_{cf}, a second matching step is used to search for corresponding points in P_{cf}. Then, in order to ensure the quality of the scan matching algorithm, the proposed approach divides the matching stage in two steps. Firstly, the matching of curvature functions is obtained in a fast way using the Fourier domain. Next, the second matching step consists of matching points from the set of corresponding curvature functions. Only these pairwise points are used to obtain the estimated displacement Δp^r.

(1) *Matching of the curvature functions associated to the current and reference laser scans.* Once the curvature

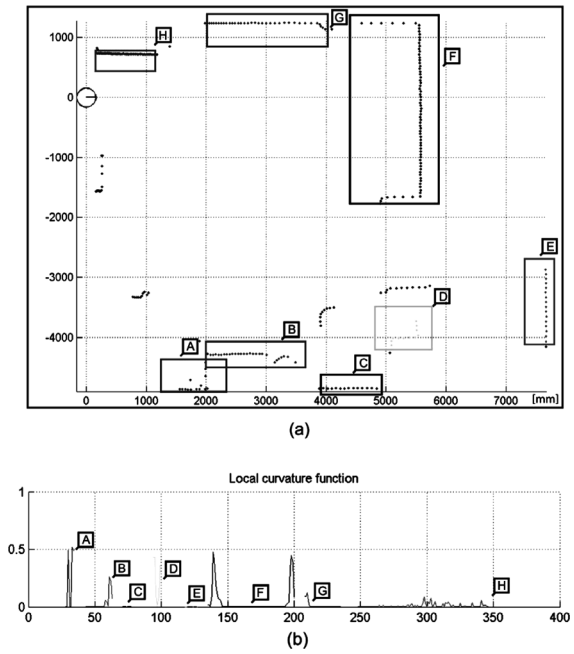


Fig. 4. CF-SMA1 description: (a) The environment scan is segmented using the distance-based criterion and (b) curvature functions of each segment are computed. In this case, $N_c = 8$.

https://doi.org/10.1017/S0263574708004840 Published online by Cambridge University Press

functions associated to each group of the reference scan R and current scan C have been obtained (Section 2.1), a matching is performed between both the sets to obtain a first estimation of the transformation that maps C onto R. This transformation will roughly correspond to the movement of the robot between the acquisition of these scans. To match these two sets of curvature functions, a matrix of possible matching pairs is built. The element υ_{ij} of this matrix is defined by the similarity measure between two curvature functions. A fast way to measure the similarity of two curvature functions is to work on the Fourier domain, where correlations are transformed into products.[1] In order to achieve this transformation with a low computational time, FFT is used. It implies that the length of each curvature function must be previously normalized to a value of 2^n (e.g. 64, 128 or 256). Then, the correlation index or distance function, υ_{ij}, is defined as

$$\upsilon_{ij} = IFFT(FFT[c_i] \cdot FFT[r_j])_{i=1,\ldots,N_c, j=1,\ldots,N_r}, \quad (6)$$

where IFFT is the Inverse Fast Fourier Transform, and $c_i \in C_{cf}$ and $r_j \in R_{cf}$. When all correlation indexes have been calculated, the maximum value of this correlation matrix is found for each row ($\upsilon_{ij}^{\max}$) and the corresponding curvature functions of C and R are matched if this value is higher than a previously defined threshold U_c. This value U_c is imposed to eliminate matched curvature functions with a low value of correlation index. The described process is iteratively applied to obtain a set of pairwise curvature functions, $P_{cf} = \{p_k = (c_i, r_j)_k \,|\, c_i \in C_{cf}, r_j \in R_{cf}, \upsilon_{ij} = \max\{\upsilon_{in} \,|\, n = 1, \ldots, N_l^r\}, k = 1, \ldots, N_k\}$, where N_k is the number of matched curvature functions.

(2) *Matching pairwise points from the set of corresponding curvature functions.* Each point of a curvature function has an associated range reading. Thus, the set of pairwise curvature functions, P_{cf}, defines a set of N_t' possible matched points, $M_{cf}^{t'}$. Let $m_l^c = \{(x_l, y_l)\}_{l=1,\ldots,N_{t'}}$ be the set of range readings associated to the matched curvature functions of the current scan. In the same way, let $m_l^r = \{(x_l, y_l)\}_{l=1,\ldots,N_{t'}}$ be the set of range readings associated to the matched curvature function of the reference scan. Therefore, $M_{cf}^{t'} = \{(m_l^c, m_l^r) \,|\, m_l^c, m_l^r \in \mathbb{R}^2, l = 1, \ldots, N_{t'}\}$. In order to reduce and to improve the quality of the matching process, this second step will select and match only N_t range readings from the set of N_t' possible matched points, $M_{cf}^{t} \subseteq M_{cf}^{t'}$. The selection of these N_t points is based on the detection of characteristic points on the curvature function. A point of the curvature function is a characteristic one if its value is higher than a fixed threshold U_p, and is also a local maximum in the curvature function, that is

$$\begin{aligned} \eta_i &= \vartheta_{i+1} - \vartheta_i \geq U_p \\ \eta_{i-1} &< \eta_i \geq \eta_{i+1}. \end{aligned} \quad (7)$$

Figure 5 shows a fragment of the scan presented in Fig. 4 and the associated curvature function. For this scan, in Fig. 5b, the algorithm detects two characteristic points (values of curvature function upon U_p). Range readings $A = (x_a, y_a)$ and $B = (x_b, y_b)$ marked in Fig. 5a are associated to

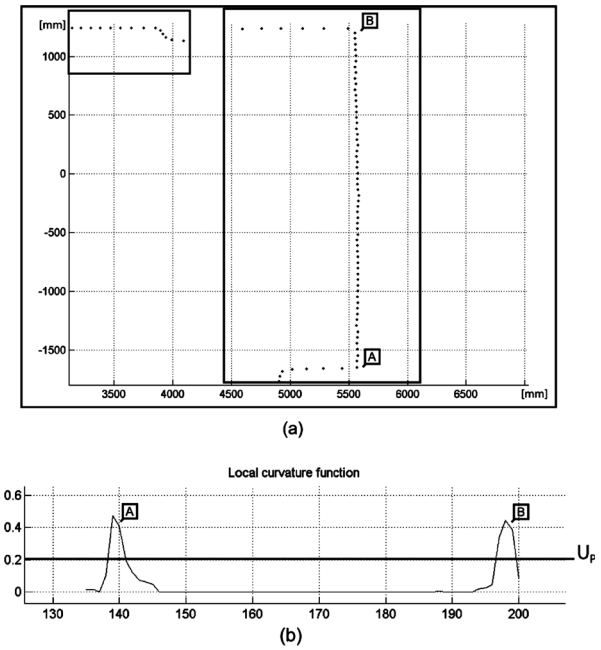


Fig. 5. (a) Fragment of a laser scan captured by the 2-D laser range finder and (b) curvature function associated to scan (a). Two characteristic points are detected and marked (A and B).

the characteristic points detected on the curvature function shown in Fig. 5b.

Let N_l^c and N_l^r be the number of characteristics points for the current and reference scan, respectively. For each pairwise curvature functions a matching between each characteristic point, $m_i^c = \{(x_i, y_i)\}_{i=1,\ldots,N_l^c}$ and $m_j^r = \{(x_j, y_j)\}_{j=1,\ldots,N_l^r}$, and a similarity coefficient, $S(m_i^c, m_j^r)$, is computed. This similarity coefficient is based on the Pearson correlation and it is obtained using the n neighbouring points on the left and right sides of the characteristic point:

$$S(m_i^c, m_j^r) = \left| S(m_i^c, m_j^r)_x \cdot S(m_i^c, m_j^r)_y \right|, \quad (8)$$

where $S(m_i^c, m_j^r)_x$ and $S(m_i^c, m_j^r)_y$ are the Pearson coefficients for the x and y co-ordinates, respectively,

$$\begin{aligned} S(m_i^c, m_j^r)_x &= \frac{\sum_{k=1}^{n} (x_{ik}^c - \bar{x}_i^c)(x_{jk}^r - \bar{x}_j^r)}{\sqrt{\sum_{k=1}^{n} (x_{ik}^c - \bar{x}_i^c)^2 \cdot (x_{jk}^c - \bar{x}_j^r)^2}}, \\ S(m_i^c, m_j^r)_y &= \frac{\sum_{k=1}^{n} (y_{ik}^c - \bar{y}_i^c)(y_{jk}^r - \bar{y}_j^r)}{\sqrt{\sum_{k=1}^{n} (y_{ik}^c - \bar{y}_i^c)^2 \cdot (y_{jk}^r - \bar{y}_j^r)^2}} \end{aligned} \quad (9)$$

being (x_i^c, y_i^c) and (x_j^r, y_j^r) the Cartesian co-ordinates for each point (c and r indicate current and reference scan, respectively), $(\bar{x}_i^c, \bar{y}_i^c)$ and $(\bar{x}_j^r, \bar{y}_j^r)$ the average values for the set of n points. $S(m_i^c, m_j^r)$ is a positive value in the range from 0 (there is no correlation) to 1 (both scans are equal). In order to improve this second matching step, the algorithm rejects candidates that satisfy these conditions:

https://doi.org/10.1017/S0263574708004840 Published online by Cambridge University Press

(a) *Low strength.* This concept is detected when $S(m_i^c, m_j^r) \leq S_{\min}$, being $S_{\min}$ a threshold which is used to eliminate candidates with low correlation index.
(b) *Low distinctiveness.* There exists m_l^r satisfying $S(m_i^c, m_l^r)/S(m_i^c, m_j^r) \approx 1$. In other words, those candidates that have similar Pearson coefficients are rejected, reducing the ambiguity in the matching process.
(c) *Unidirectionality.* For m_m^c, the match maximizing $\{S(m_m^c, m_j^r)\}_{j=1,\ldots,N_l^r}$ is $\hat{m}_n^r$, but for this latter one, the match maximizing $\{S(m_i^c, m_n^r)\}_{i=1,\ldots,N_l^c}$ is $\hat{m}_p^c \neq \hat{m}_m^c$.

Therefore, the final process obtains a set of N_l matched characteristic points. Finally, around each characteristic point, the algorithm defines a range of n matched points at right and left sides. These N_t pairwise points ($N_t = N_l(2n+1)$), constitute the set of final matched points, $M_{cf}^t = \{(m_l^c, m_l^r) |\, m_l^c, m_l^r \in \mathbb{R}^2, l = 1, \ldots, N_t\}$. The robustness and accuracy of the proposed method is based on these two described matching steps. Figure 6 shows two fragment of consecutive scans and their associated curvature functions. Matched points of these curvature functions are presented in Fig. 6b. Corresponding Cartesian co-ordinates points are marked in Fig. 6a. In this case, $N_t = 65$ and $N_l = 2$ (being n value equal to 30. Obviously, the N_t value depends on the number of data points on the left and right sides of the characteristic points).

2.3. CF-SMA3. Calculation of the relative translation and rotation

The purpose of the matching process described in Section 2.2 is to provide a set of good quality matches which allows to calculate the estimated pose of the robot. Two constraints are imposed to an optimal scan matching algorithm: (i) to be fast and (ii) to be accurate in the matching process in order to avoid mistakes in the calculation of the relative displacement.

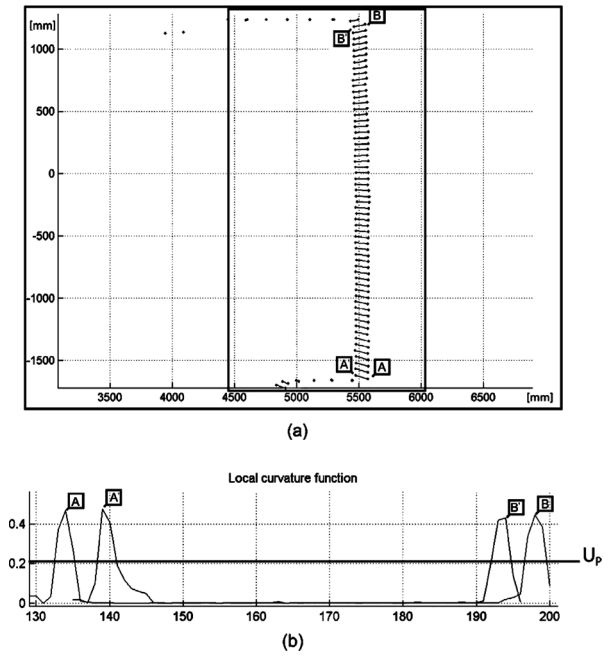


Fig. 6. (a) Two consecutive laser scans and matched points ($N_t = 65$) and (b) matching of curvature functions associated to scan (a).

These two constraints are solved using the two matching steps defined in Section 2.2. Besides, the proposed method obtains an optimal transformation for mapping the current scan onto the reference scan using a closed form solution. In this way, the algorithm minimizes the displacement error without iterations, improving the computational cost.[9]

The solution of this problem consists of solving the minimization of the error function:

$$E(R_{\Delta\theta}, \Delta T) = \sum_{i=1}^{N_t} \sum_{j=1}^{N_t} \omega_{ij} \left\| m_i^c - \left(R_{\Delta\theta} m_j^r + \Delta T\right) \right\|^2, \tag{10}$$

where m_i^c and m_j^r are the matched range readings belonging to M_{cf}^t, and ω_{ij} is a binary value defined as 1 if m_i^c and m_j^r have been matched or 0 if they have not been matched. $R_{\Delta\theta}$ and ΔT are the searched rotation and translation matrices which relate the current and reference scans. They are defined as

$$R_{\Delta\theta} = \begin{pmatrix} \cos\Delta\theta^r & \sin\Delta\theta^r \\ -\sin\Delta\theta^r & \cos\Delta\theta^r \end{pmatrix}, \tag{11}$$

$$\Delta T = \begin{pmatrix} \Delta x^r \\ \Delta y^r \end{pmatrix}, \tag{12}$$

where $\Delta p^r = (\Delta x^r,\ \Delta y^r,\ \Delta\theta^r)^T$ describes the estimated relative shift which allows to estimate p_{t+1}^r from p_t^r. An extended development of the optimization problem described in Eq. (10) is detailed in ref. [9]. In that work, authors obtain a closed-form expression which allows to compute the rotation and translation matrices according to the set of matched points, instead of employing an iterative minimization algorithm. Thus, after computing the pose shift Δp^r as the optimal transformation, the robot pose is updated using the Eq. (1) and the current scan is saved as a new reference scan ($C \longleftarrow R$). Convergence of the solution is ensured due to the non-iterative method used by the scan matching algorithm to estimate the robot displacement.[9]

Finally, to correctly integrate the scan matching process into other navigation tasks, such as a SLAM algorithm, it is necessary to know the statistical properties of the estimate robot displacement, Δp^r. Thus, in SLAM, the probability error distribution associated to the proposed approach is needed to use the pose provided by the scan matching algorithm in the SLAM stochastic process. This error distribution is considered as Gaussian noise, and it is represented by a covariance matrix, which indicates the quality of the pose estimation. In fact, high values on the main diagonal of the covariance reflects an increase in the uncertainty. In order to obtain the error covariance matrix of the pose estimation, the technique described by Lu and Milios[10] is used. In this work, the theory of linear regression is applied on a scan matching algorithm to derive the covariance matrix of the robot displacement analytically. Equation (10) defines a non-linear error function of the displacement ($R_{\Delta\theta}$, ΔT), where the non-linearity is due to the robot rotation, $\Delta\theta^r$.

Let (x_i^c, y_i^c) and (x_i^r, y_i^r) be the Cartesian co-ordinates of two matched points, that is, both data point denote the same

https://doi.org/10.1017/S0263574708004840 Published online by Cambridge University Press

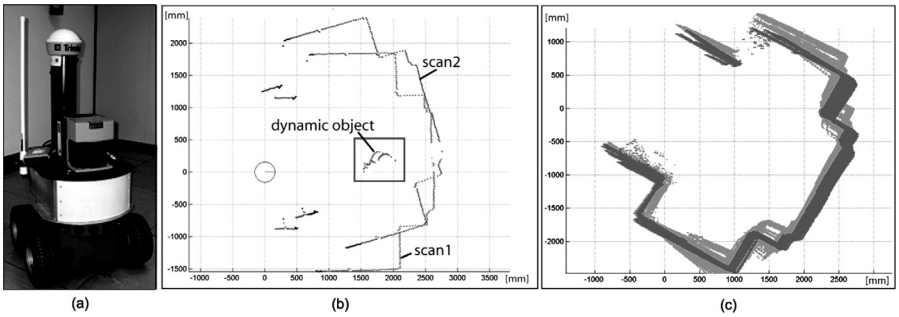


Fig. 7. (a) Pioneer 2-AT robot equipped with a LMS200 laser sensor; (b) one example of current and reference scans used for the first experiment (see text for details) and (c) resulting maps after testing the proposed algorithm in the second experiment (dark grey color). Map based on the odometry information (light grey).

point in the real scene. Therewith Eq. (10) simplifies to

$$E(R_{\Delta\theta}, \Delta T) = \sum_{i=1}^{N_t} \left\| m_i^c - \left(R_{\Delta\theta} m_i^r + \Delta T \right) \right\|^2 \qquad (13)$$

which can be linearized for small $\Delta\theta^r$ values[†], as

$$\begin{aligned} &\begin{pmatrix} x_i^c \\ y_i^c \end{pmatrix} - \begin{pmatrix} \cos(\Delta\theta^r) & \sin(\Delta\theta^r) \\ -\sin(\Delta\theta^r) & \cos(\Delta\theta^r) \end{pmatrix} \begin{pmatrix} x_i^r \\ y_i^r \end{pmatrix} - \begin{pmatrix} \Delta x^r \\ \Delta y^r \end{pmatrix} \\ &\approx \begin{pmatrix} x_i^c \\ y_i^c \end{pmatrix} - \begin{pmatrix} 1 & \Delta\theta^r \\ -\Delta\theta^r & 1 \end{pmatrix} \begin{pmatrix} x_i^r \\ y_i^r \end{pmatrix} - \begin{pmatrix} \Delta x^r \\ \Delta y^r \end{pmatrix} \\ &\Rightarrow \begin{pmatrix} x_i^c - x_i^r \\ y_i^c - y_i^r \end{pmatrix} - \begin{pmatrix} 1 & 0 & y_i^r \\ 0 & 1 & -x_i^r \end{pmatrix} \begin{pmatrix} \Delta x^r \\ \Delta y^r \\ \Delta\theta^r \end{pmatrix} \\ &= (Y - M\hat{b})^T (Y - M\hat{b}) \end{aligned} \qquad (14)$$

being $\hat{b} = (\Delta x^r, \Delta y^r, \Delta\theta^r)^T$, the estimate robot displacement, and M and Y are defined as

$$\begin{aligned} Y &= \begin{pmatrix} x_i^c - x_i^r \\ y_i^c - y_i^r \end{pmatrix}, \\ M &= \begin{pmatrix} 1 & 0 & y_i^r \\ 0 & 1 & -x_i^r \end{pmatrix}. \end{aligned} \qquad (15)$$

The above equation is linear, and thus, it is possible to use the linear regression analysis to calculate an optimal estimate of the covariance matrix associated to the robot displacement[10]:

$$C_{R_{\Delta\theta}\Delta T} = (M^T M)^{-1} \sigma^2 \qquad (16)$$

being σ^2 the variance of the measurement laser error, supposing Gaussian with zero mean. In ref. [10], the authors propose an estimate of the σ^2 value:

$$\sigma^2 = \frac{1}{N_t - 3} \cdot E_{\min}(\hat{b}), \qquad (17)$$

where $E_{\min}(\hat{b})$ is the minimum error according to the estimate robot displacement $\hat{b}$. Thus, the covariance matrix of the estimator $\hat{b}$ is a 3×3 symmetric matrix whose diagonal elements are the variances of the three-parameter estimator and whose off-diagonal elements are their correlations:

$$C_{R_{\Delta\theta}\Delta T} = \begin{pmatrix} \sigma^2_{\Delta x^r} & \sigma_{\Delta x^r \Delta y^r} & \sigma_{\Delta x^r \Delta\theta^r} \\ \sigma_{\Delta x^r \Delta y^r} & \sigma^2_{\Delta y^r} & \sigma_{\Delta y^r \Delta\theta^r} \\ \sigma_{\Delta x^r \Delta\theta^r} & \sigma_{\Delta y^r \Delta\theta^r} & \sigma^2_{\Delta\theta^r} \end{pmatrix}. \qquad (18)$$

3. Results

The described scan matching algorithm has been tested in various real environments. Our Pioneer 2-AT robot is equipped with a SICK Laser Measure System LMS200 and an embedded Pentium III-1000 MHz. The field of view is 180° in front of the robot and up to 8 m distance. The range samples are spaced 0.5°, all within the same plane. Figure 7a shows the robot used in the experiments.

The experiments are focused on the evaluation of the proposed method in terms of robustness, accuracy and processing time in dynamic environments. Besides, a comparative study with the main scan matching algorithms has been provided. Previously, this section explains how the parameters of the proposed algorithm have been adjusted.

3.1. Estimation of parameters

The proposed method requires choosing values for a set of parameters. The main parameters described in this paper are:

1. The parameters σ_ρ and λ used by the breakpoints detector.
2. The threshold value which determines the noise level tolerated by the adaptive curvature detector, U_k.
3. The minimum correlation index value to be considered as pairwise curvature functions, U_c.
4. The parameter U_p, defined as the minimum value of a curvature function to be considered as a characteristic point of the scan laser.

[†]Typical values for $\Delta\theta^r$ are small due to the frequency of acquisition of consecutive laser scans.

https://doi.org/10.1017/S0263574708004840 Published online by Cambridge University Press

5. The number of points at right and left sides of the characteristic point used by the closed form to determine the relative displacement, n.
6. The threshold $S_{\min}$ which rejects pairwise characteristic points with low strength.

As was described in Section 2.1, the process to obtain the values for σ_ρ and λ is based on the previous work of Borges and Aldon.[4] These values have been fixed to 0.005 m and 10°, respectively.

The threshold value U_k is used to eliminate spurious noise of the laser scan. In order to set it correctly, a set of real plane surfaces has been scanned at different distances from the robot. In these planar surfaces, the values must be fixed to do not detect any local peak. This simple experiment has provided a U_k value equal to 1.0. This value has been used in the experiments described in this paper.

A similar experimental process has been used to obtain the values for U_c and U_p. The first one is employed to improve the correlation process, thus pairwise curvature functions whose associated correlation index is lower than U_c are discarded (residual noise in the FFTs). On the other hand, U_p is used to detect characteristic points of the laser scan. In this case, a set of real surfaces has been scanned at different distances. In these situations, the values must be fixed to match both, the curvature functions and to detect most of the characteristic points of the scans. From this test, U_c and U_p values have been fixed to 0.4 and 0.2 rad, respectively.

Next, the value of n is calculated. It must be noted that a low value of n implies few points to be used in Eq. (8) and thus, estimated pose results can be inaccurate. On the contrary, a high value of n includes too much points in the estimation process, increasing the computational load of the algorithm. In short, the value of n must be selected taking into account these situations. After several tests where the ground truth was known, it has been found that an n value equal to 30 reduces the displacement errors at an acceptable computation time.

Finally, the threshold $S_{\min}$ value was selected to 0.2. To do that, a set of consecutive scans has been considered at different robot position (distance and orientation). The matching process between characteristic points was analysed with details, $S_{\min}$ being selected in order to reject pairwise points with small correlation value which would be wrong solution.

3.2. Experiments with ground truth

The experiments reported in this section focus on two aspects of the estimation performance: the accuracy of the displacement estimates and the robustness with respect to errors due to dynamic objects in the scene. To test the proposed algorithm, two experiments are achieved. The first experiment consists of matching two consecutive scans acquired in the same robot location, $(x^r, y^r, \theta^r)^T = (0, 0, 0)^T$, the difference being between one scan to another due to the sensor's noise and the presence of people moving in the robot surrounding. Next, to the second scan is applied a random rotation and translation (the average values of the random translation and rotation are 100 cm and 15° respectively, with standard deviation $\sigma_x^r = \sigma_y^r = 50$ mm and $\sigma_\theta^r = 5°$ (see Fig. 7b). After applying the experiment 1000 times in this scenario, the final average displacement error was limited to $\Delta x^r = 12$ mm, $\Delta y^r = 22$ mm and $\Delta\theta^r = 0.12°$. In this particular case, the average number of matched points N_t associated to the set of pairwise curvature functions was 245.

The second experiment compares the overall accuracy of the algorithm. The experiment consists of a set of consecutive scan (1100 scans) acquired in a static environment. The robot was tele-operated with small displacements (rotations and translations) around its initial position $p_{t=0}^r = (0, 0, 0)$. Finally the robot was stopped and the final location (pose and orientation) was measured with an uncertainty less than 2 mm in displacement and 0.2° in orientation. The true robot pose at the end of the experiment was $x_a^r = 46$ mm, $y_a^r = 52$ mm and $\theta_a^r = 4.38°$. Results of the estimate robot pose were $x^r = 29$ mm, $y^r = 26$ mm and $\theta^r = 3.9°$. Figure 7c illustrates the resulting map after applying the proposed scan matching algorithm (dark grey color) and the resulting map only using the odometric information (light grey color).

3.3. A comparative study

Given the settings and specifications described in Section 3.1, the Pioneer 2-AT robot has been tele-operated into two different indoor scenarios: the research area at the Telecommunication Engineering School (University of Málaga) and the ISIS Group Laboratories at the Andalusian Technology Park (Málaga). The first test area is used to test the described approach in a static environment, meanwhile in the second experiment some people were walking around the robot, simulating a dynamic environment. The comparative study is based on the accuracy, robustness, processing time and easiness of the implementation. The methods used in this comparative study have been provided by Gutmann's implementation (see ref. [7] for more details): Iterative Dual Correspondence (IDC), Cox Algorithm[5] and Histogram scan matching.[16] IDC consists of matching raw data of both scans without features detection, e.g. all points of the scans are used on the matching process. The matching problem is solved by two rules: the closest point rule and the matching range rule. On the contrary, Cox Algorithm extracts lines from reference scan and subsequently matches data points of current scan to these lines. Finally, the Histogram scan matching defines an angle and x-y histograms from both scans and compare them using a cross correlation function. The covariance matrix of the robot displacement estimate is directly provided by Gutmann's implementation, which uses the same method described in ref. [10]. This was one of the reasons to use this method in the proposed scan matching algorithm (Section 2.3). Thus, the displacement estimate error of the proposed approach is easily compared with the other scan matching algorithms of this comparative study.

Figure 8 shows the results of the proposed method for the first test area. The experiment was made up of 325 consecutive scans where the robot moves along approximately 60 meters. The collected data was analysed by the different scan matching algorithms. As is illustrated in Fig. 8a-d, IDC, Cox and the proposed algorithm have similar results, although Cox algorithm presents a slight orientation error. On the other hand, Histogram method is

https://doi.org/10.1017/S0263574708004840 Published online by Cambridge University Press

Table II. Accuracy and average time comparison of scan matching algorithms in the first test area (Fig. 8).

Algorithm	Runtime t (ms)	$p^r_{t=\text{end}}$			Covariance matrix		
		x^r (mm)	y^r (mm)	θ^r (rad)	$\sigma^2_{\Delta x^r}$ (mm^2)	$\sigma^2_{\Delta y^r}$ (mm^2)	$\sigma^2_{\Delta\theta^r}$ (rad^2)
Proposed method	5.21	−7219.3092	−23283.6090	−3.1280	43.5973	28.9805	$1.11\cdot10^{-6}$
IDC	9.76	−7269.3092	−24113.6090	−3.1280	93.5973	8.9805	$1.17\cdot10^{-6}$
Cox	6.01	−6304.4608	−24214.2705	−3.0854	3.6642	7.6670	$1.21\cdot10^{-6}$
Histogram	36.87	−7351.9021	−16347.9748	3.1285	105.3965	217.13	$4.05\cdot10^{-6}$

not an accurate method in this test area and the robot pose estimate suffers from abrupt errors. Table II compares the accuracy of the approach and the average time needed to calculate the overall trajectories from the static environment described in this section. In this table, $\Delta p^r = (x^r, y^r, \theta^r)^T$ describes the final robot pose estimate, $\sigma^2_{\Delta x^r}$, $\sigma^2_{\Delta y^r}$ and $\sigma^2_{\Delta\theta^r}$ represent the average values of the main diagonal of the covariance matrix associated to the robot displacement estimate. Table III describes the maximum values of the main diagonal covariance matrix along the robot trajectory, $\sigma^2_{\Delta x^r{}_{\max}}$, $\sigma^2_{\Delta y^r{}_{\max}}$ and $\sigma^2_{\Delta\theta^r{}_{\max}}$. Tables II and III allow to compare the accuracy of the proposed method with respect to the classic scan matching algorithms for this first experiment. Finally, Fig. 8a-d shows the resulting map provided by each one of the scan matching algorithms.

The second experiment presents people moving through the robot trajectories. The robot moves approximately 80 m where it acquires 525 consecutive scans. Results of the proposed approach for this test area are shown in Fig. 9. There are not additional corrective algorithms in this experiment and the results are obtained directly by the proposed method. It must be noted that dynamic objects are also represented in the figure (grey points), but this information has been correctly discarded by the proposed algorithm. Figure 9b illustrates the trajectories calculated by different algorithms, including the proposed approach. Table IV compares the average time needed to calculate the trajectories from the dynamic environment described in this section. Besides,

Table III. Maximum errors in the first test area (Fig. 8).

Algorithm	Maximum errors		
	$\sigma^2_{\Delta x^r{}_{\max}}$ (mm^2)	$\sigma^2_{\Delta y^r{}_{\max}}$ (mm^2)	$\sigma^2_{\Delta\theta^r{}_{\max}}$ (rad^2)
Proposed method	79.2312	44.71	$1.45\cdot10^{-7}$
IDC	133.6036	45.0509	$1.94\cdot10^{-7}$
Cox	29.9873	23.2671	$2.01\cdot10^{-6}$
Histogram	108.1252	254.5831	$5.90\cdot10^{-6}$

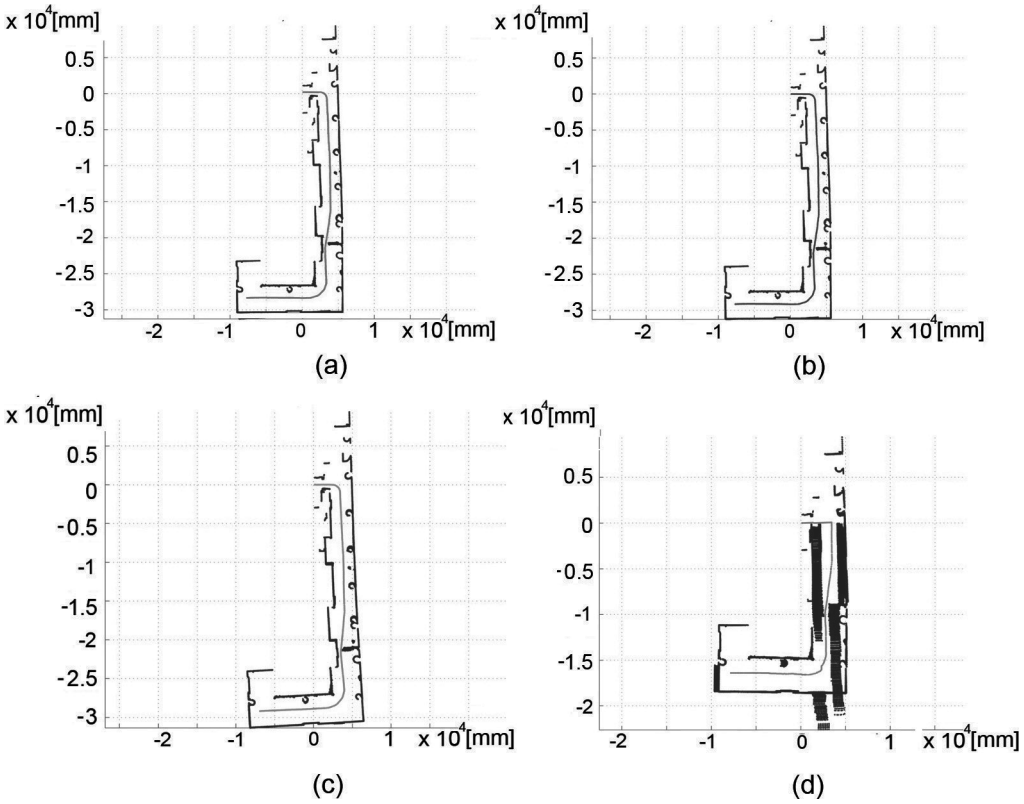


Fig. 8. Scan matching algorithms comparative study: (a) Proposed Algorithm; (b) the IDC algorithm; (c) Cox's algorithm; and (d) the histogram scan matching approach.

https://doi.org/10.1017/S0263574708004840 Published online by Cambridge University Press

Table IV. Accuracy and average time comparison of scan matching algorithms in the first test area (Fig. 9).

Algorithm	Runtime t (ms)	$p^r_{t=\text{end}}$			Covariance matrix		
		x^r (mm)	y^r (mm)	θ^r (rad)	$\sigma^2_{\Delta x^r}$ (mm^2)	$\sigma^2_{\Delta y^r}$ (mm^2)	$\sigma^2_{\Delta\theta^r}$ (rad^2)
Proposed method	6.12	2631.8370	−4112.3917	−3.1280	9.7225	18.9105	$0.3198 \cdot 10^{-6}$
IDC	11.77	1921.3812	−2889.4661	3.0397	44.1961	17.4872	$1.56 \cdot 10^{-6}$
Cox	7.81	2722.7021	−4087.1654	−3.02666	9.1273	9.7877	$0.3966 \cdot 10^{-6}$
Histogram	47.21	7168.9900	−2729.3401	−3.1181	225.0112	731.3500	$7.01 \cdot 10^{-6}$

Table V. Maximum errors in the second test area (Fig. 9).

Algorithm	Maximum errors		
	$\sigma^2_{\Delta x^r_{\max}}$ (mm^2)	$\sigma^2_{\Delta y^r_{\max}}$ (mm^2)	$\sigma^2_{\Delta\theta^r_{\max}}$ (rad^2)
Proposed method	228.1331	154.7112	$1.35 \cdot 10^{-7}$
IDC	303.5510	460.7651	$1.92 \cdot 10^{-6}$
Cox	279.1355	162.5655	$1.36 \cdot 10^{-7}$
Histogram	220.111	637.7621	$7.08 \cdot 10^{-6}$

Table VI. Easiness of the implementation comparative: Number of parameters needed to be tuned.

	τ
Proposed method	7
IDC	4
Cox	5
Histogram	2

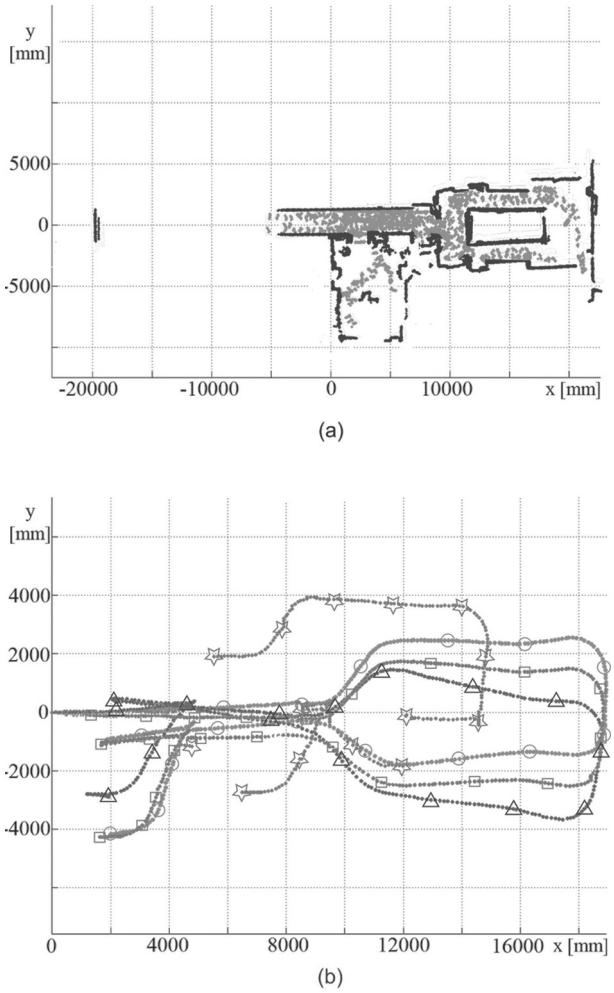


Fig. 9. Scan matching algorithms comparative study: (a) Resulting map obtained with the proposed algorithm in the second test area and (b) trajectories computed by algorithms applied in this comparative study. (Square: proposed method, circle: Cox's solution, triangle: IDC algorithm and star: Histogram approach.)

Tables IV and V summarize the numerical results of the accuracy of each scan matching algorithm similar to Tables II and III. It can be appreciated that the proposed algorithm is computationally faster and accurate than the other methods. This is due to the non-iterative nature of the algorithm and due to the fact that it uses a few but accurate matched points for the calculation of the relative displacement. Robustness to dynamic objects in the scene and possible correspondence errors is improving in the described scan matching algorithm, as can be appreciated in Fig. 9b.

Finally, Table VI compares the easiness of each implementation (defined as the number of parameters in the algorithm needed to be tuned, τ). Classic IDC approach and Cox's algorithm employ as input parameters the maximum number of iterations and the minimum error which describes the convergence of the method (translation and rotation minimum errors). Besides, both the methods include a set of filters to improve the results (a projection filter and a median filter, basically). Finally, Cox's method uses a line extraction method for making the Cox algorithm suitable for the scan matching. On the other hand, Histogram scan matching algorithm also includes a line extraction method for reducing errors due to isolated peaks in the histogram associated to measurement errors. Then, it only needs to apply histograms to the consecutive scans in order to estimate the displacement. In this comparative study, only those parameters which describe a correct operation of the algorithms have been taken into account. As was commented in Section 3.1, the designer has to select values for the distinct scan matching steps in order to obtain a reliable set of matched points. For this reason, the proposed approach needs to set more parameters ($\tau = 7$) than the other approaches. These parameters are easy to design and their values are selected according to the explanation described in Section 3.1. However, there are some considerations to be taken into account, since the success of the proposed approach depends on the number of

https://doi.org/10.1017/S0263574708004840 Published online by Cambridge University Press

points which takes part in the matching process and this value is dependent on some parameters (e.g. U_p, n or $S_{\min}$). The experiments described in this section demonstrate that the correct selection of these values leads to acceptable operation in different environments.

4. Conclusions

This paper proposes a new scan matching approach which computes the transformation between the current and the reference scans in three stages. Firstly, a segmentation stage is conducted to divide the whole scan in a set of segments associated to physical entities of the robot surrounding. Then, the curvature function associated to each segment is computed according to a modified algorithm of the previous work presented in ref. [13]. Curvature functions are invariant with respect to rotation and translation and they can be quickly computed. Therefore, the second stage of the approach matches curvature functions of both scans providing a global estimation of the scan matching. Next, the algorithm chooses characteristic points in corresponding curvature functions as features to estimate the final robot pose shift. Finally, the use of a closed-form solution to calculate the updating of the pose and the definition of pairwise points using curvature functions improve the computational load of the complete algorithm. Besides, the uncertainty of the estimate robot displacement is provided in order to test the accuracy of the approach.

We have implemented and tested the technique in several experiments, in order to measure the robustness, accuracy and computational time of the whole scan matching algorithm. The approach has been compared with other classic scan matching algorithms into real dynamic and static environments (IDC, Cox and Histogram methods provided by Gutmann's implementation[7]). According to the comparative study results, the described approach improves these classic scan matching algorithms working in static and dynamic environments in accuracy, robustness and time processing. Future works are focused on the implementation of a SLAM algorithm using the pose information estimate and on testing it in a dynamic and unstructured environment.

Acknowledgements

We would like to thank the Steffen Gutmann's scan matching implementations for the comparative study section. The authors would also like to thank the anonymous referees for their suggestions and insightful comments. This work has been partially granted by the Spanish Ministerio de Educación y Ciencia (MEC) and FEDER funds, Project n. TIN2005-01359 and by the Junta de Andalucía Project n. P07-TIC-03106.

References

1. A. Bandera, C. Urdiales, F. Arrebola and F. Sandoval, "On-line Unsupervised Planar Shape Recognition based on Curvature Functions," *24th Annual Conference of the IEEE Industrial Electronics Society (IECON'98)*, Aachen, Germany (1998), Vol. 3, pp. 1268–1272.
2. O. Bengtsson and A. J. Baerveldt, "Robot localization based in scan-matching estimating the covariance matrix for the IDC algorithm," *Robot. Autonom. Syst.* **44**(4), 29–40 (2003).
3. J. L. Blanco, J. A. Fernández-Madrigal and J. A. González, "Approach for Large-Scale Localization and Mapping: Hybrid Metric-Topological SLAM," in *IEEE International Conference on Robotics and Automation*, Rome Italy (2007) pp. 2061–2067.
4. G. A. Borges and M. Aldon, "Line extraction in 2-D range images for mobile robotics," *J. Intell. Robot. Syst.* **40**, 267–297 (2004).
5. I. J. Cox, "Blanche—an experiment in guidance and navigation of an autonomous robot vehicle," *IEEE Trans. Robot. Automation*, **7** (2), 193–204 (1991).
6. M. Dissanayake, P. Newman, S. Clark, H. Durrant-Whyte and M. Csorba, "A solution to the simultaneous localisation and map building problem," *IEEE Trans. Robot. Automation* **17** (3), 229–241 (2001).
7. J. S. Gutmann and C. Schlegel, "AMOS: Comparison of Scan Matching Approaches for Self-Localization in Indoor Environments," in *1st Euromicro Workshop on Advanced Mobile Robots*, Kaiserslautern, Germany (1996) pp. 61–67.
8. D. Hähnel, D. Fox, W. Burgard and S. Thrun, "A highly efficient FastSLAM algorithm for generating cyclic maps of large-scale environments from raw laser range measurements," in *IEEE/RSJ International Conference on Intelligent Robots and Systems*, Las Vegas, Nevada, USA. (2003) pp. 206–211.
9. K. Lingemann, A. Nuchter, J. Hertzberg and H. Surmann, "High-speed laser localization for mobile robots," *Robot. Autonom. Syst.* **51**(4), 275–296 (2005).
10. F. Lu and E. E. Milios, "Robot pose estimation in unknown environments by matching 2-D range scans," *Technical Report No. RBCV-TR-94-46*, pp. 8–12. University of Toronto, Toronto (1994).
11. M. Montemerlo, FastSLAM: A Factored Solution to the Simultaneous Localization and Mapping Problem with Unknown Data Association *Ph.D. Thesis* (Carnegie Mellon University, 2003), Pittsburgh, Pensilvania, USA.
12. J. Nieto, T. Bailey and E. Nebot, "Recursive scan-matching SLAM," *Robot. Autonom. Syst.* **55**, 39–49 (2007).
13. P. Núñez, R. Vázquez-Martín, J. C. del Toro, A. Bandera and F. Sandoval, "Natural landmark extraction for mobile robot navigation based on an adaptive curvature estimation," *Robot. Autonom. Syst.* **56**(3), 247–264 (2008).
14. S. Pfister, Algorithms for Mobile Robot Localization and Mapping, Incorporating Detailed Noise Modeling and Multi-Scale Feature Extraction *Ph.D. Thesis* (California Institute of Technology, 2006), Pasadena, California, USA.
15. C. C. Wang, C. Thorpe and S. Thrun, "Online simultaneous localization and mapping with detection and tracking of moving objects: Theory and results from a ground vehicle in crowded urban areas," *Proceedings of the IEEE International Conference on Robotics and Automation (ICRA)*, Taipei, Taiwan (2003) pp. 842–849.
16. G. Weiss and E. Puttkamer, "A map based on laser scans without geometric interpretation," *Intell. Autonom. Syst.* **4** 403–407 (1995).

https://doi.org/10.1017/S0263574708004840 Published online by Cambridge University Press